Available online at www.sciencedirect.com

SCIENCE DIRECT

Thin Solid Films 469–470 (2004) 372–376

thin solid films

www.elsevier.com/locate/tsf

Boron–carbide barrier layers in scandium–silicon multilayers

A.F. Jankowski*, C.K. Saw, C.C. Walton, J.P. Hayes, J. Nilsen

Lawrence Livermore National Laboratory, P.O. Box 808, MS L-352, Livermore, CA 94551-9900, United States

Available online 22 October 2004

Abstract

Scandium–silicon (Sc/Si) multilayer structures show promise to efficiently reflect 45–50-nm wavelength X-rays at normal incidence. Barrier layers have been added at each interface to minimize the formation and growth of silicide compounds that broaden interfaces and, consequently, cause a change in the layer spacing and loss of reflectivity. Although tungsten (W) is an effective diffusion barrier, its high absorption causes a loss of reflectivity. We now evaluate the use of another refractory material for the barrier layer, boron carbide (B_4C), which is a stable ceramic. The multilayer microstructure and its stability are evaluated using microscopy and diffraction methods. It is found that the use of B_4C enhances the thermal stability of Sc/Si multilayers to an extent equivalent that offered by W barrier layers with only a few percent reduction in the reflectivity.

Keywords: Boron–carbide; Multilayer; Scandium–silicon; Diffusion barrier; Reflectivity

1. Introduction

Silicon-based multilayers, for example, in the form of Mo/Si mirrors have become prominent as a manufactured material of choice for deep extreme-ultraviolet (EUV) lithography [1,2]. In addition, Mo/Si mirrors are routinely used to manipulate laboratory X-ray laser beams that operate in the 13–24-nm wavelength range—an example of which is the X-ray laser interferometer that operates at 14.7 nm [3]. There has been a search for high-reflectivity, optical coatings that work in longer wavelength regimes since the demonstration of the Ne-like Ar, tabletop X-ray laser that operates at 46.9 nm. This capillary-discharge Ar laser has achieved saturated laser operation with outputs of 1 mJ per pulse and has been operated at a 4-Hz repetition rate [4]. Also, experiments at the Compact Multi-pulse Terawatt (COMET) laser facility at Lawrence Livermore National Laboratory have demonstrated a laser-driven Ar laser that operates at 46.9 and 45.0 nm using a gas puff target [5]. Recent investigations show that Sc/Si multilayer structures can efficiently reflect X-rays at a 47-nm wavelength as generated from a laser source and can function over the 35–50-nm wavelength range [6,7]. Thus, Sc/Si multilayers offer a potential application for the effective manipulation of compact discharge and laser-driven X-ray laser (XRL) beams at normal incidence and at 45° incidence.

Artificially, composition-modulated structures such as Sc/Si are intrinsically metastable and subject to interdiffusion [8,9]. The metastability of Si-based multilayer structures to interdiffusion subsequently leads to the formation and growth of silicide compounds that broaden interfaces and consequently cause a change in the layer spacing and loss of reflectivity. So, despite some initial success, the Sc and Si layers were found to interdiffuse at temperatures above 150–200 °C that lowered the reflectivity. To address the problem of a change in layer spacing, thin tungsten layers less than 1 nm thick were deposited at each interface to serve as diffusion barriers [10]. Unfortunately, the use of tungsten adversely affects the reflectivity of the multilayer mirror due to adsorption. The reflectivity measured at normal incidence of a 20-nm multilayer decreased by half its peak value with the addition of tungsten barrier layers.

There is a need to develop deposition processes to stabilize the interfaces of Sc/Si multilayer structures that can

* Corresponding author. Tel.: +1 925 423 2519; fax: +1 925 422 0049.
E-mail address: jankowskil@llnl.gov (A.F. Jankowski).

0040-6090/$ - see front matter © 2004 Elsevier B.V. All rights reserved.
doi:10.1016/j.tsf.2004.08.153

be used in the UV range near 45 nm. An alternate material choice is now presented to serve as a diffusion barrier based on prior substitutive use of boron carbide to stabilize carbon-based multilayer structures [11–13]. In these studies, B_4C proved to be thermally stable in multilayer structure with W and maintain compositionally abrupt interface structure. In comparison, W/C multilayers degraded in performance and structure even when subjected to low temperature anneal treatments. In addition, a B_4C interlayer should sustain a higher reflectivity due to lower absorption of light, smoothness and distinct interfaces. Recently, B_4C has been used as a barrier layer to improve the stability and reflectivity of Mo/Si multilayers by reducing interface silicide formation [14]. Thus, we now propose to use B_4C as a barrier layer to prevent interdiffusion between each Sc and Si layer. Results are presented for the synthesis and structural characterization of 17–25-nm repeat period Sc/Si multilayers with and without B_4C barrier layers.

2. Experimental methods

2.1. Synthesis

Planar magnetron sputtering was implemented to deposit the Sc/Si-based multilayer structures. Magnetron sputtering functions by attracting an ionized inert gas such as Ar through a magnetic field to the cathode surface, i.e. the target held at a negative potential. As the Ar^+ ions hit the target, they erode the surface and cause sputtered neutrals to diffuse to the substrate surface. Polished fused quartz substrates of 9.5–25.4 mm diameter are used as substrates for the reflectivity measurements along with silicon wafers for cross-section microscopy examination. In the deposition system (shown in Fig. 1), the multilayers were deposited by sequentially rotating the substrates to the 3-cm diameter sputtering targets of Si, B_4C and Sc as operated in the dc mode. The deposition chamber is cryogenically pumped to a base pressure of 10^{-6} Pa. The source-to-substrate separation is 10.2 cm. The discharge voltage of the sources ranged from 290 V for Sc to 480 V for B_4C. A working gas pressure of pure Ar at 1.3 Pa is flowed at a rate of 30 $cm^3 \cdot min^{-1}$.

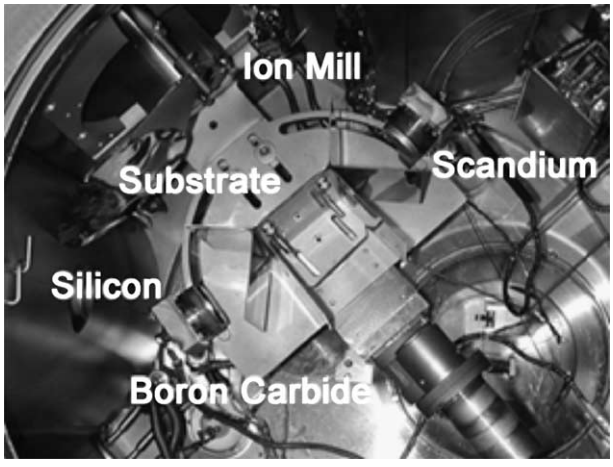

Fig. 1. A top view is shown of the sputter deposition chamber.

Prior to deposition, a short exposure to a 3-cm diameter Ar^+ ion beam was used for an in-situ pre-clean of the fused-quartz substrate surface. The ion gun (shown in Fig. 1) was operated with a 700-V beam voltage for several minutes to remove 10–20 nm of substrate material. The three deposition sources were shielded from each other in order to avoid cross-contamination. Calibrated quartz-crystal monitors were used to monitor the individual deposition rates and total thickness accumulation from the targets. The deposition rates are 0.016, 0.083 and 0.181 $nm \cdot W^{-1} \cdot min^{-1}$ for the source materials of B_4C, Si and Sc, respectively. The Sc layers are deposited at a thickness equivalent to 36% of the layer pair spacing. Twenty layer pairs are deposited for each multilayer sample.

After deposition, several of the multilayer deposits are subjected to isothermal anneal treatments. The multilayer-coated fused quartz substrates are annealed at 200 °C under a vacuum of 10^{-4} Pa for periods of time totaling 2 and 6 h. A transient of 5 min from 50 to 200 °C occurs on heating and cool down using a quartz lamp heater.

2.2. Characterization

X-ray diffraction characterization is carried out at grazing incidence and glancing angle. The multilayer films are characterized using a powder diffractometer with Cu $K\alpha$ X-ray radiation. The high-angle diffraction scans reveal the presence of any long-range ordering. To maximize the amount of sample irradiated by the X-ray beam, these scans are taken at a glancing angle of incidence. Data acquisition is carried out using a curved position sensitive detector. The grazing angle scans are taken in the $\theta/2\theta$ mode and reveal the satellite reflections indicating the nature of the composition fluctuation to the multilayer. The positions of the satellites through the n^{th} order of reflection are used to fit the repeat period of the multilayer using Bragg's Law. Details of the fitting procedure that includes correction for refraction are given in Section 3. For the reflectivity measurements conducted at the Advanced Light Source at Lawrence Berkeley Laboratory, the samples are scanned over a wavelength range that spanned from 20 to 28 nm. The 95% s-polarized incident beam was positioned at 45° (θ) relative to the substrate surface.

Imaging of a cleaved multilayer structure in cross-section is carried out using atomic force microscopy (AFM). The sample is coated with a layer of enamel prior to cleaving since the multilayer is located at the surface of the substrate and the probe tip could fall off the edge during scanning. In contact mode, the AFM functions by moving a probe tip along the sample surface and mapping its features. The probe tip is attached to a cantilever that deflects a different amount depending on the height of the surface features. A

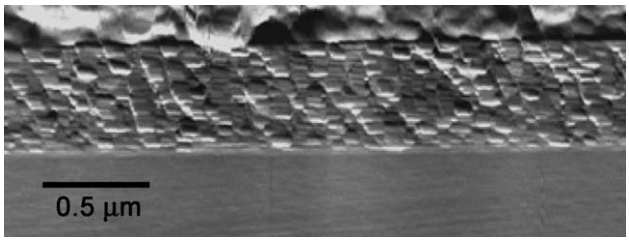

Fig. 2. A contact-mode deflection image of a 26-nm $Sc/B_4C/Si/B_4C$ multilayer as viewed in cross-section.

laser is directed at the cantilever and its deflection is measured as the laser hits a photodetector. A horizontal resolution of 2 nm can be achieved using this technique. In addition to the AFM, imaging of samples in cross-section is carried out using transmission electron microscopy (TEM). The samples for TEM are mechanically thinned and ion milled to produce a cross-section less than 50 nm thick that is suitable for imaging in bright field and at high resolution. Selected area diffraction patterns are taken to reveal the crystalline state (or lack thereof) of the imaged region.

3. Results and analysis

3.1. Microstructure

The cross-section AFM image of a 25-nm repeat period $Sc/B_4C/Si/B_4C$ multilayer is shown in Fig. 2 [15]. The 20 layer pairs of the structure are visible above the substrate surface along as are columnar-features that are likely associated with fracture morphology. (The enamel layer caps the top of the multilayer.) The image may contain a dimensional skew as a result of the cross-section slope that might cause some level of layer distortion. The high angle X-ray diffraction scans contain no Bragg reflections indicating the structure of the Sc, Si and B_4C layers are amorphous and/or *nano*-crystalline. The lack of apparent crystalline structure in the as-deposited state is confirmed through TEM analysis. The bright field image (shown in Fig. 3a) reveals the microstructure as viewed in cross-section and confirms that the Sc layers are deposited at a thickness equivalent to 36% of the layer pair spacing. The diffraction pattern (seen as the Fig. 3a insert) only contains the superlattice reflections about the incident beam that are indicative of the composition modulation. There are no diffraction spots indicating the lack of crystalline structure within the layers. The high-resolution image (shown in Fig. 3b) again indicates the layers are amorphous.

3.2. Reflectivity

The reflectivity of two 20-layer pair Sc/Si multilayers with and without 0.7-nm-thick B_4C interfacial layers (in Fig. 4) show near equivalent peak reflectivities of 25–26% over the incident X-ray wavelength range of 19.5–29.5 nm. Using the fitting procedure provided by the Windt IMD code—a dynamical model based on recursive application of the Fresnel equations [16,17], the reflectivity is calculated at normal incidence. The predicted maximum reflectivity of the 19.6-nm repeat period multilayer with the B_4C barrier layers at 37.2-nm wavelength is only 12% less than the 70% reflectivity predicted for the 18.1-nm repeat period Sc/Si multilayer at 36.5-nm wavelength, as based on the measurements at 45° incidence. The sharpness of all the Sc–Si interfaces, as fitted to the multilayer spectra in Fig. 4, are 2.3 nm with the B_4C barrier layers and 2.8 nm without the barrier layers. Although the normal incidence reflectivity is less using the B_4C layers (with some of the difference being attributable to the longer repeat period), the decrease is much less than the 50% loss when using W barriers layers (reported by Vinogradov et al.) in a similar 20-nm repeat period, Sc/Si-based multilayer [10].

3.3. Stability

The stability of the multilayer structures are evaluated using X-ray diffraction after the isothermal anneal treatments at 200 °C. Experimental results for 8.048 keV Cu $K\alpha$ X-rays are shown in Fig. 5 for the 20.5-nm repeat

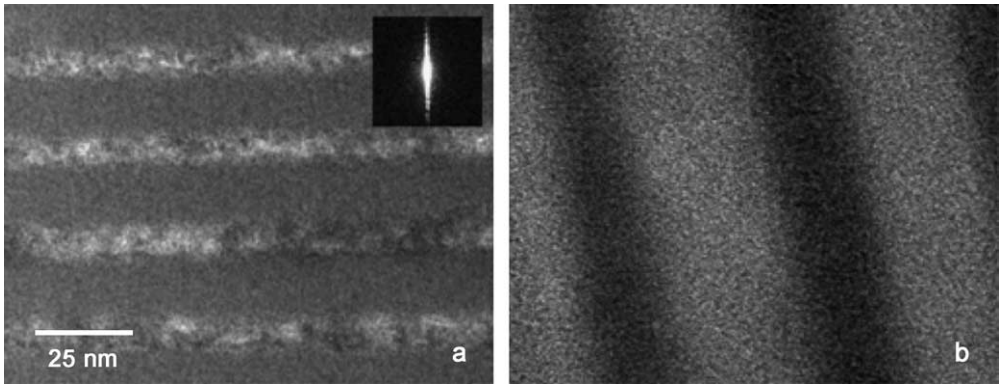

Fig. 3. Transmission electron microscopy reveals the microstructure of the 25-nm repeat period $Sc/B_4C/Si/B_4C$ multilayer as viewed in cross-section under (a) bright field and (b) high-resolution imaging conditions.

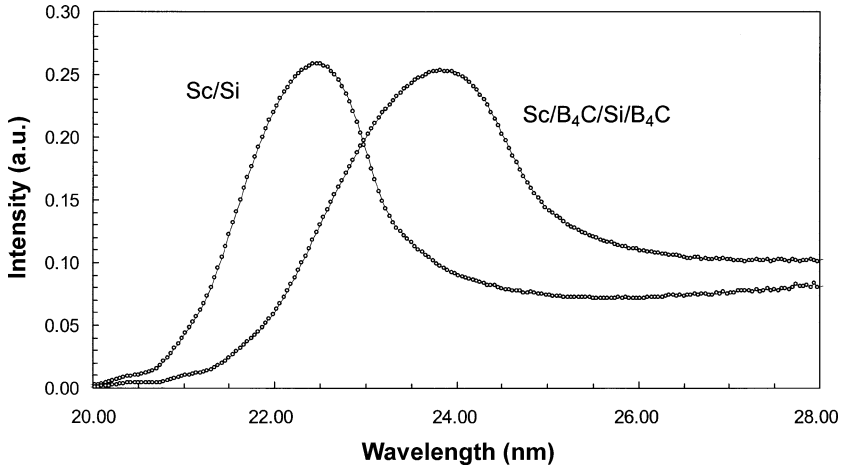

Fig. 4. The measured reflectivity of Sc/Si and Sc/B_4C/Si/B_4C multilayers at 45° incidence.

period Sc/Si multilayer and in Fig. 6 for the 18.8-nm repeat period Sc/B_4C/Si/B_4C multilayer with the 0.7-nm-thick B_4C interface layers in both the as-deposited condition (t=0 h) and after the anneal treatments. The 2-h anneal decreases the repeat period of the Sc/Si multilayer by 11% (from 20.5 to 18.2 nm), whereas the Sc/B_4C/Si/B_4C multilayer decreases by only 5% (from 18.8 to 17.9 nm repeat period). After a total time of 6 h at 200 °C, all but the first-order satellite reflection of the Sc/Si multilayer (curve not shown) have decayed to such a large extent that prohibits an accurate fit of the repeat period. This indicates that the interfacial diffusion process has nearly homogenized the composition fluctuation of the Sc/Si multilayer. However, no discernable changes in the repeat period or relative intensity of satellites are observed (as shown in Fig. 5) for the Sc/B_4C/Si/B_4C multilayer as the anneal treatment progresses from 2 h to a total time of 6 h. It appears that the multilayer structure with the interfacial B_4C barrier layers has equilibrated at 200 °C. In comparison, Vinogradov et al. [10] found that a 21.8-nm repeat period Sc/Si multilayer decreased by 4% after a 1-h anneal at 200 °C and by 2% after a 2-h anneal at 150 °C. These results are consistent with the present findings in that the Sc/Si multilayer structure is unstable for low-temperature anneal treatments. For the Sc/Si multilayers with a 0.8-nm-thick W barrier layers, the 22.9-nm repeat period structure decreased by <1% after a 1-h anneal at 200 °C [10]. The present results are comparable with regards to the improved stability through the use of an interfacial barrier layer noting the anneal times at 200 °C are longer in the present study. Future work will require a quantitative assessment of changes in the multilayer reflectivity with annealing in addition to the present findings regarding the stability of the multilayer periodicity.

4. Summary

Sc/Si multilayers offer a potential application for the effective manipulation of compact-discharge, laser-driven X-ray laser beams. However, degradation of the mirror reflectivity can occur since the structure of the Sc/Si multilayer is metastable when subjected to anneal treat-

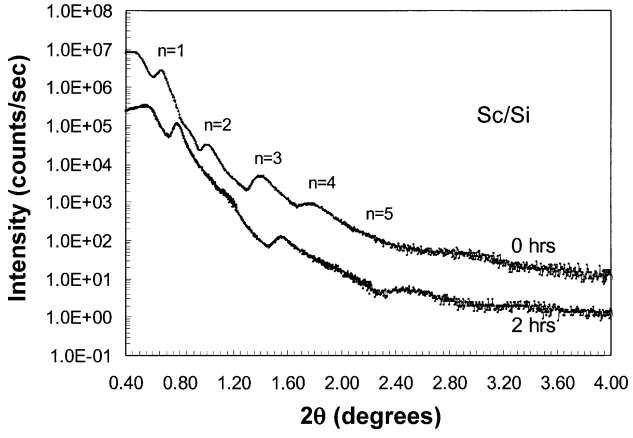

Fig. 5. The measured reflectivity of a Sc/Si multilayer in the as-deposited condition (t=0 h) and after a 2-h anneal at 200 °C.

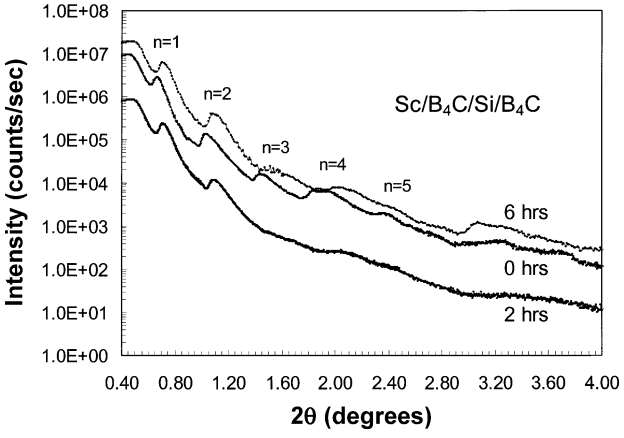

Fig. 6. The measured reflectivity of a Sc/B_4C/Si/B_4C multilayer in the as-deposited condition (t=0 h), after a 2- and 6-h anneal at 200 °C.

ments. The use of nanometer-thin B_4C barrier layers is shown to help stabilize the interface structure by reducing the amount of change in the repeat period after 200 °C anneal treatments. The reflectivity decreases by only a few percent when the B_4C barrier layers are added to each interface of the base Sc/Si mirror.

Acknowledgment

The authors thank Jennifer Harper and Rich Gross for their efforts in transmission electron microscopy. This research was supported through the Laboratory Directed Research and Development program under project no. 03-FS-003. This work was performed under the auspices of the U.S. Department of Energy by the University of California, Lawrence Livermore National Laboratory under contract no. W-7405-Eng-48.

References

[1] T.W. Barbee Jr., S. Mrowka, M.C. Hettrick, Appl. Opt. 24 (1985) 883.
[2] D.G. Stearns, P.B. Mirkarimi, E. Spiller, Phys. Rev. Lett. 446 (2004) 37.
[3] R.F. Smith, J. Dunn, J. Nilsen, V.N. Shlyaptsev, S. Moon, J. Filevich, J.J. Rocca, M.C. Marconi, J.R. Hunter, T.W. Barbee Jr., Phys. Rev. Lett. 89 (2002) 065004.
[4] C.D. Macchietto, B.R. Benware, J.J. Rocca, Opt. Lett. 24 (1999) 1115.
[5] J. Dunn, R.F. Smith, J. Nilsen, H. Fiedorowicz, A. Bartnik, V.N. Shlyaptsev, J. Opt. Soc. Am. B 20 (2003) 203.
[6] A. Yu., Uspenskii, V.E. Levashov, A.V. Vinogradov, A.I. Fedoenko, V.V. Kondratenko, Yu.P. Pershin, E.N. Zubarev, V.Yu. Fedetov, Opt. Lett. 23 (1998) 771.
[7] I.A. Artioukov, B.R. Benware, J.J. Rocca, M. Forsythe, Yu.A. Uspenskii, A.V. Vingradov, IEEE J. Sel. Top. Quantum Electron. 5 (1999) 1495.
[8] A. Jankowski, T. Tsakalakos, Mater. Sci. Eng. B, Solid-State Mater. Adv. Technol. 6 (1990) 87.
[9] A.L. Greer, F. Spaepen, in: L.L. Chang, B.C. Giessen (Eds.), Synthetic Modulated Structure Materials, Academic Press, New York, NY, p. 419.
[10] A.V. Vinogradov, Yu. P. Pershin, E.N. Zubarev, D.L. Voronov, A.V. Pen'kov, V.V. Kondratenko, Yu. A. Uspenskii, I.A. Artioukov, J.F. Seely, SPIE Proceedings 4505 (2001) 230.
[11] A.F. Jankowski, D.M. Makowiecki, Opt. Eng. 30 (1991) 2003.
[12] A.F. Jankowski, L.R. Schrawyer, M.A. Wall, J. Appl. Phys. 68 (1990) 5162.
[13] A.F. Jankowski, L.R. Schrawyer, M.A. Wall, D.M. Makowiecki, J. Vac. Sci. Technol. A 7 (1989) 2914.
[14] S. Bajt, J.B. Alameda, T.W. Barbee Jr., W.M. Clift, J.A. Folta, B. Kaufmann, E.A. Spiller, Opt. Eng. 41 (2002) 1797.
[15] L. Friedman, A.F. Jankowski, Characterization of Sc/Si multilayers using atomic force microscopy, Lawrence Livermore National Laboratory, Summer Research Symposium, 2003, UCRL-MI-154707.
[16] D.L. Windt, F.E. Christensen, W.W. Craig, C. Hailey, F.A. Harrison, M. Jimenez-Garate, R. Kalyanaraman, P.H. Mao, J. Appl. Phys. 88 (2000) 460.
[17] D.L. Windt, R. Hull, W.K. Waskiewicz, J. Appl. Phys. 71 (1992) 2675.